Supporting Information

Rotem et al. 10.1073/pnas.1004333107

SI Text

Determining the Plating Efficiency of Different Strains. Cells were diluted $1:10^2$–$1:10^3$ and grown in LB, at 37 °C, in 24-well plates, in a Wallac VICTOR® reader until $OD_{630} \sim 0.2$. Inducer was added at the required concentration and cfu assayed 3 h later, when cells were diluted in $1:10^6$–$1:10^7$ and plated on LB agar plates with the appropriate antibiotics.

FRET Measurements. TH1433R cells (Table S1) all bearing the pzS21Venus-HipB plasmid controlling Venus-HipB fusion protein under the *tet* promoter, as well as three variants of the HipA and mCherry on the pBAD33 plasmids: (*i*) HipA-mCherry fusion protein, (*ii*) HipA7-mCherry fusion protein, and (*iii*) *HipA* + free mCherry. Cells were plated on LB-agarose pads with 0.06% arabinose and 30 ng/mL atc. A light-emitting diode illumination system with intensity stability (PreciseExcite, CoolLED) was used for imaging the donor Venus-HipB fluorescence level. Four consecutive pictures were acquired at 1 s intervals before and after bleaching >90% of acceptor fluorescence (mCherry) by 7.5 s illumination with a mercury lamp through mCherry excitation filter. Comparisons between the FRET signals of the different strains were done within the same experiments.

Lag Measurements Using Microscope Cells were grown and induced similarly to the scanner measurements and plated on agarose pads comprising 1.5% agarose + M9 + 15 μg/mL ampicillin. Low level of ampicillin ensures that growing bacteria eventually die so that late growers can be detected without being overwhelmed by nearby growing bacteria. The pads were put under the microscope at 37 °C. During the first hour of the experiments, fluorescence and phase-contrast images were taken every 7–10 min. After the first hour, only phase-contrast images were taken. Cells with different induction levels of *hipA* were measured in parallel during the same experiment, and several locations of each condition were monitored.

Media and Reagents. All experiments were performed at 37 °C. Cells were grown in LB (BD) or in M9 (BD) + 0.1% 1 M $MgSO_4 \bullet 7H_2O$ + 0.005%B1(Thiamine) + 0.1%casamino acids+ 0.4%glucose. For pBAD33 plasmids, glycerol was added instead of glucose, as well as arabinose 0–0.4%. Anhydrous tetracycline (atc) 0–40 ng/mL was purchased from Acros Organics. Appropriate antibiotics (Sigma) were added as follows: chloramphenicol 25 μg/mL, kanamycin 30 μg/mL, and ampicillin 15 μg/mL or 100 μg/mL.

Microscopy. Microscopy was performed using a Leica DMIRE2 inverted microscope system with automated stage (Ludl) and shutters (Uniblitz) and controlled temperature box (Life Imaging Systems). Autofocus and image acquisition were done using custom macros in Scope-Pro (Media Cybernetics). Images were acquired with a 100× oil objective, a cooled CCD camera (Orca ER, Hamamatsu) and processed using Matlab (The Mathworks) and ImageJ [National Institutes of Health (NIH)]. Fluorescence was measured using high-quality filters (Chroma): Venus, HQ500/20x + HQ535/30m; mCherry, HQ575/50x + HQ640/50m.

Strains and Plasmids Construction. MG1655Δ (MG1655 deleted of *hipB* and *hipA* genes) was generated by gene disruption and fusion as described in ref. 1 using hipp1, hipp2, c1, c2, nb15′, and nb13′ primers (Table S3).

pZS21B was constructed by PCR amplification of *hipB* from the chromosome of MG1655 using BxbaIR and BxbaIF primers and ligation into the XbaI site of the pZS21 plasmid.

pzS2HGFP was constructed by PCR amplification of the *hip* promoter from the chromosome MG1655 using HXHOH1 and HECOH primers and ligation in the EcoRI and XhoI enzymes of the pZS21GFP (2) plasmid.

Plasmid pZA21A + mCherry was constructed for the current work by subcloning of 1323-bp DNA fragment containing *hipA* ORF into pZA21mCherry. At first step, *hipA* was amplified by PCR on pBAD33-A plasmid with primers pZA21-hipA FWD and pZA21-hipAstop REV. Amplified hipA fragment was restricted by *EcoRI* and introduced into pZA21mCherry.

pBAD33*hipA*-mCherry was constructed by subcloning of 1416-bp DNA fragment containing the *hipA* sequence without stop codon and added 3′-linker sequence and 725 bp DNA fragment containing mCherry sequence without start codon. These were introduced into pBAD33 by two-step cloning. At first, *hipA* was amplified by PCR on pBAD33*hipA* plasmid with primers pBAD-F and 3-hipA-int1, and introduced into BamHI-XbaI site of pBAD33 to produce pBAD33*hipA*(-stop) + linker. In the second step, mCherry was amplified by PCR from plasmid pRSET-BmCherry with primers 5-cher-int2 and 3-cher-ext2, and introduced into XbaI-SphI site of pBAD33*hipA*(-stop) + linker plasmid.

pBAD33*hipA7*-mCherry was constructed by subcloning of 1416-bp DNA fragment containing full-length *hipA7* sequence without stop codon and additional linker sequence introduced into pBAD33*hipA*-mCherry. For this purpose *hipA7* was amplified by PCR on pBAD33*hipA7* plasmid with primers pBAD-F and 3-hipA-int1, and introduced into BamHI-XbaI site of pBAD33*hipA*-mCherry instead of *hipA*.

pBAD33*hipA* + mCherry was constructed by subcloning of mCherry sequence with additional 5′-linker and RBS into pBAD33*hipA* plasmid. For this purpose 734-bp DNA fragment of mCherry sequence was amplified by PCR on pRSET-BmCherry with primers FWD-mCher-SphI and Rev-mCher-SphI and introduced into the SphI site of pBAD33*hipA* plasmid.

Western Blot Assay. Comparative expression analysis of the fusion HipA-mCherry and HipA7-mCherry proteins was performed according to following procedure: Bacteria were collected by 3 min centrifugation at 6,800 × *g*. After centrifugation, proteins were extracted by vortex and 5 min boil in SDS-PAGE sample buffer (63 mM Tris-HCl, pH 6.8, 10% glycerol, 5% β-mercaptoethanol, 2% SDS, and 0.0025% Bromophenol blue). Protein concentration was determined by Coomassie staining of total proteins separated by SDS-PAGE. For Western blotting, samples containing equal amounts of total proteins were loaded onto a 15% SDS polyacrylamide gel and SDS electrophoresis was performed using standard procedure. For immunoblot analyses, proteins were transferred to nitrocellulose membranes using a gel blotter (Bio-Rad). Western blotting was performed with Living Colors® DsRed Polyclonal Antibodies (Clontech) according to instructions of the manufacturer. The goat anti-rabbit secondary antibody conjugate (Jackson Human Research, Inc.) was used in 1:5,000 dilution. A SuperSignal® West Pico Pirce chemiluminescent detection kit (Thermo Scientific) was used for protein detection.

Persistence Measurements. Cells were grown in LB with different amounts of arabinose, at 37 °C, in 24-well plates, in Wallac

VICTOR® reader. After entering stationary phase cells were diluted and plated on LB plates placed in the scanner to detect cfu appearance. In order to test persistence to antibiotic treatment, the cells were diluted 1 : 100 into LB + ampicillin. After 3 h, they were diluted again, plated on Petri dishes, and put on the scanner.

Pearson's Coefficient Evaluation. For evaluating Pearson's coefficient, the pixels corresponding to each bacterium were automatically detected according to the phase-contrast image. For each bacterium, the correlation between the intensities in the red fluorescence channel and the green fluorescence channel were computed using Pearson's coefficient formula. Thus, a value of Pearson's coefficient was assigned to each bacterium in the population separately. The mean Pearson's coefficient for the colocalization of mCherry and Venus was significantly higher in mCherry fused to HipA when compared to the fusion to HipA7 ($p < 0.05$) or to free mCherry in the control cells ($p < 0.05$).

Analysis was done using ImageJ (NIH) and Matlab (The Mathworks).

1. Haldimann A, Wanner BL (2001) Conditional-replication, integration, excision, and retrieval plasmid-host systems for gene structure-function studies of bacteria. *J Bacteriol* 183:6384–6393.
2. Guet CC, Elowitz MB, Hsing WH, Leibler S (2002) Combinatorial synthesis of genetic networks. *Science* 296:1466–1470.

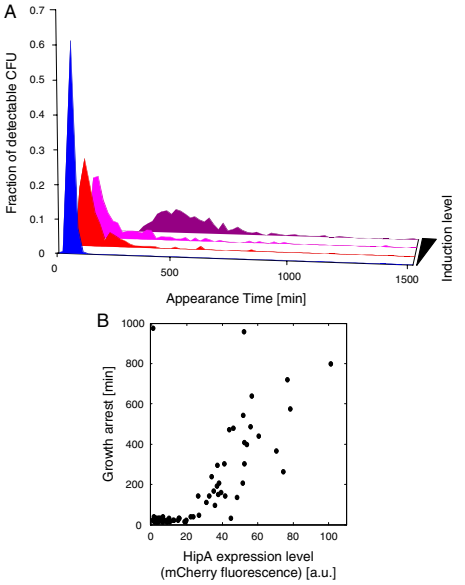

Fig. S1. HipA expression in the presence of endogenous HipB results in a transient growth arrest—experiments using the arabinose promoter in pBAD33*hipA* + mCherry in MGN bacteria (*hipB*$^+$). (*A*) Bacteria were grown in batch cultures and plated on LB plates after 3 h of HipA induction at different levels: blue, no induction; red, low induction; magenta, medium induction; violet, high induction. The histograms show the fraction of cfu detected at each time point. Growth-arrested bacteria are detected at later times. High levels of HipA result in long and widely distributed growth arrest times. (*B*) Measurement of lag time of single bacteria using time-lapse microscopy shows the correlation between the amount of HipA expression (indicated by the fluorescence level of mCherry) and the growth arrest time. Each point represents the growth arrest duration of one bacterium, and its fluorescence at $t = 0$. Below a threshold level of HipA expression, most of the bacteria have a short growth arrest. Zero fluorescence is defined as the background of cells not expressing mCherry.

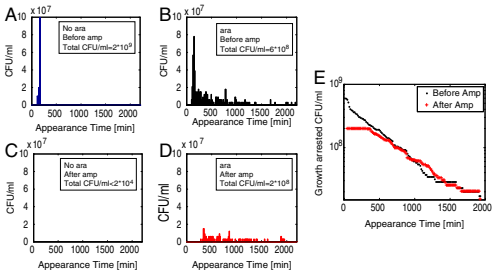

Fig. S2. Persistence to antibiotic treatments following HipA expression is due to the growth-arrested bacteria. (*A* and *B*) Appearance of colonies on plates for bacterial cultures of pBAD33*hipA* MGN without (*A*), or after induction of *hipA* with arabinose (*B*). HipA expression results in a tail of growth-arrested cells. (*C* and *D*) The same cultures as in *A* and *B* were exposed to 2 h of ampicillin treatment and plated at appropriate dilutions. No cfu were detected in cells that did not express HipA. More than 30% survival was observed for cells expressing HipA. Note that the peak of bacteria that are not growth arrested in *B* has disappeared after the ampicillin treatment in *D*. Only the growth-arrested tail survives. (*E*) Same data as in *B* (black) and *D* (red) replotted as one minus the cumulative density function, showing that the cells that survived the antibiotic treatment belong to the tail of growth-arrested cells.

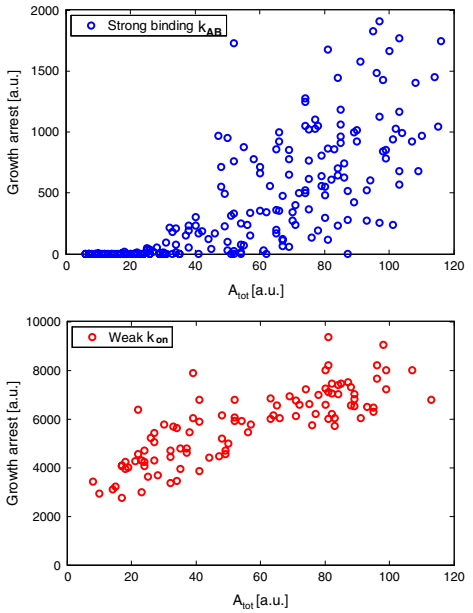

Fig. S3. High k_{AB} binding constant is required for the coexistence of different time scales. Computer simulation results of our model (Fig. 3*A*) with different values of k_{AB}. (*A*) When k_{AB} is in the regime of strong binding, coexistence of growth-arrested and normally growing cells is observed. (*B*) When k_{AB} is lowered (by 2 orders of magnitude), either by decreasing the binding rate (k_{on}) (*B*), or by increasing the unbinding rate (k_{off}), the result is a uniform distribution of growth-arrest times.

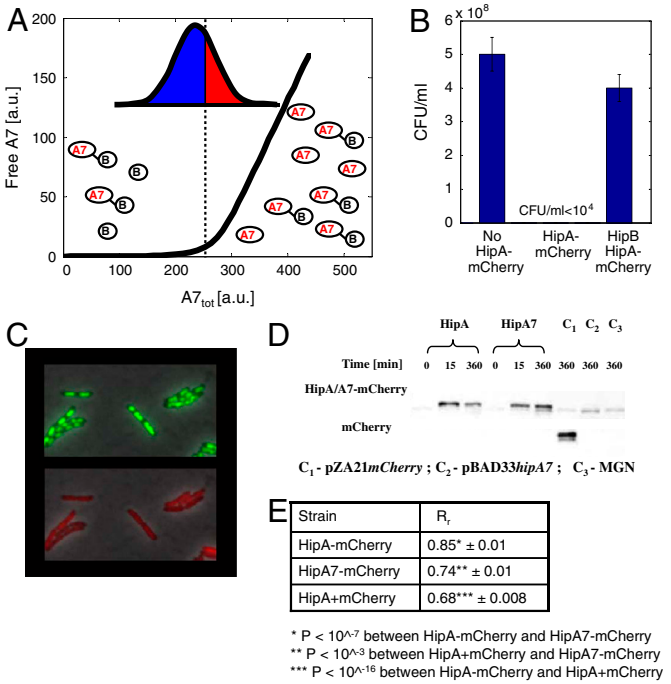

E

Strain	R_r
HipA-mCherry	0.85* ± 0.01
HipA7-mCherry	0.74** ± 0.01
HipA+mCherry	0.68*** ± 0.008

* P < 10^{-7} between HipA-mCherry and HipA7-mCherry
** P < 10^{-3} between HipA+mCherry and HipA7-mCherry
*** P < 10^{-16} between HipA-mCherry and HipA+mCherry

Fig. S4. HipA versus HipA7. (*A*) Simulation results and illustration for the amount of free HipA7 as a function of total initial HipA7 in a cell, [$A7_{tot}$]. The amount of free HipA7 is negligible until [$A7_{tot}$] reaches a threshold. Cells with $A7_{tot}$ above the threshold will be persistent (red). The A7 mutation brings the HipA7 distribution closer to the threshold and results in a higher population of growth-arrested cells (red). (*B*) The fusion protein HipA-mCherry retains its toxic activity, which can be counteracted by HipB. No cfu were retrieved from cells expressing HipA-mCherry only, showing that the fusion protein retains its toxicity. Cells expressing HipA-mCherry and HipB have the same number of colony-forming units per milliliter as cells not expressing HipA-mCherry at all. (*C*) Localization of Venus-HipB and free mCherry. Microscopy images (phase and fluorescence overlays) of cells deleted for the *hipBA* module and bearing the fusion protein Venus-HipB (green) together with expression of *HipA* + free mCherry proteins (red). The green fluorescence is localized (namely, smaller then the phase contour), whereas the red fluorescence is distributed in the entire cell, as expected, resulting in reduced colocalization (see Fig. S4*E*). (*D*) Western blot analysis shows that the fusions between the HipA/HipA7 and mCherry remain intact during growth. Columns (HipA) – pBAD33A-mCherry at different times after induction (at $t = 0$). Column (HipA7) – pBAD33A7-mCherry at different times after induction (at $t = 0$). Column C_1 – Control, pZA21mCherry at 360 min. Column C_2 – Control, pBAD33A7 at 360 min. Column C_3, cells without any plasmid at 360 min. (*E*) Colocalization evaluations of Venus-HipB and three variants of the HipA and mCherry proteins on the pBAD33 plasmids: HipA-mCherry fusion protein; HipA7-mCherry fusion protein; HipA + free mCherry. The Pearson's coefficients (R_r) shown were computed for 135, 151, and 209 single cells, respectively. The colocalization signal is the highest for the HipA-mCherry protein, and weaker for the *hipA7* mutation, suggesting reduced binding between HipA7 and HipB. Standard error of the mean is shown, as well as pairwise *p* values.

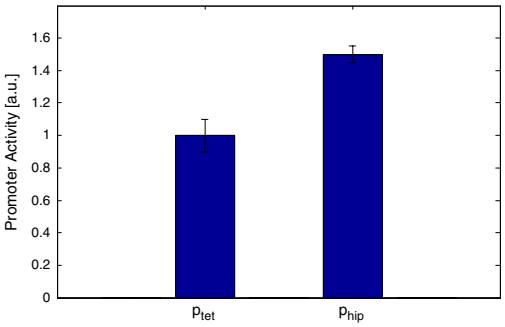

Fig. S5. Comparison between the promoter activities of P_{hip} and P_{tet}. The promoter activities of the *tet* and *hip* promoters were measured by monitoring concomitantly the fluorescence expression from the pZE21mcherry and pZE2Hmcherry plasmids, respectively. OD_{630} and mCherry fluorescence measurements (excitation at 575 nm; emission at 625 nm) were done in a shaking Wallac VICTOR® reader in 24-well plates with 200 μL of mineral oil to prevent evaporation. The background fluorescence level was determined using a strain without plasmid. We defined promoter activity (PA) as $\frac{dFluorescence}{dt} \cdot \frac{1}{OD}$.

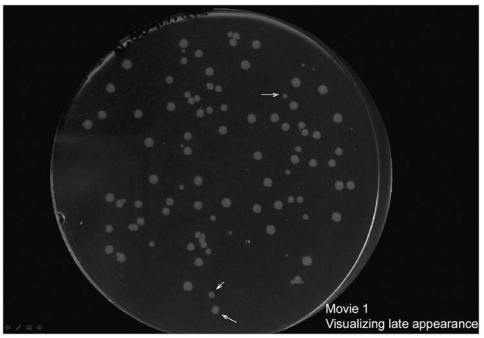

Movie S1. (Related to Fig. 2) Appearance of colonies on LB plate. The plates are automatically imaged every 15 min using a commercial scanner. The time-lapse images are then automatically analyzed for extracting the distribution of appearance of the colonies. Here, pzS21B pBAD33*hipA* TH1433 bacteria are shown. We verified by microscopic observations that the delay in appearance is indeed due to a longer growth arrest.
Movie S1 (AVI)

Table S1. Bacterial strains and plasmids

Strains and plasmids	Relevant characteristics	Source
MG1655	WT *E. coli* K-12	*E. coli* Genetic Stock Center (CGSC#7740)
HM22	F+ *dapA* zde-264::Tn*10 hipA7*	(1)
MG1655A7	MG1655 with *hipA7*; P1 of HM22 in MG1655 using Tet selection	(2)
LN3542	*hipA*::*tet*cw	(3)
MGN	MG1655 Δ*hipA::tetA*	This work
MG1655Δ	MG1655 Δ*hipBA:Cam*^{R}	This work
TH1433	MG1655 Δ*hipBA*	(4)
pZ vector system		(5)
pZA21mCherry	pZ series producing mCherry [a generous gift from Tsien's lab (6)] under *tet* promoter.	This work
pZA21A+mCherry	pZ series producing HipA and mCherry transcriptionally fused under *tet* promoter	This work
pZS21B	pZ series producing HipB under *tet* promoter	This work
pZS21VenusB	pZ series producing Venus-HipB translationally fused under *tet* promoter	This work
pBAD33*hipA*	*hipA* gene in *Eco*RI-*Pst*I sites of pBAD33	(4)
pBAD33A+mCherry	pBAD33*hipA* producing mCherry under the same promoter	This work
pBAD33A-mCherry	pBAD33*hipA* producing mCherry translationally fused	This work
pBAD33*hipA7*	*HipA7* gene in *Eco*RI-*Pst*I sites of pBAD33	(4)
pBAD33A7-mCherry	pBAD33*hipA7* producing mCherry translationally fused	This work
pZS2HGFP	pZ series producing GFP under *hip* promoter	This work
pZE2HmCherry	pZ series producing mCherry under *hip* promoter	This work
pZE21mCherry	pZ series producing mCherry under *tet* promoter	This work

1 Moyed HS, Bertrand KP (1983) Hipa, a newly recognized gene of *Escherichia coli* K-12 that affects frequency of persistence after inhibition of murein synthesis. *J Bacteriol* 155:768–775.
2 Pearl S, Gabay C, Kishony R, Oppenheim A, Balaban NQ (2008) Nongenetic individuality in the host-phage interaction. *PLoS Biol* 6:957–964.
3 Corre J, Patte J, Louarn JM (2000) Prophage lambda induces terminal recombination in *Escherichia coli* by inhibiting chromosome dimer resolution. An orientation-dependent cis-effect lending support to bipolarization of the terminus. *Genetics* 154:39–48.
4 Korch SB, Henderson TA, Hill TM (2003) Characterization of the hipA7 allele of *Escherichia coli* and evidence that high persistence is governed by (p)ppGpp synthesis. *Mol Microbiol* 50:1199–1213.
5 Lutz R, Bujard H (1997) Independent and tight regulation of transcriptional units in *Escherichia coli* via the LacR/O, the TetR/O and AraC/I-1-I-2 regulatory elements. *Nucleic Acids Res* 25:1203–1210.
6 Shaner NC, et al. (2004) Improved monomeric red, orange and yellow fluorescent proteins derived from Discosoma sp red fluorescent protein. *Nat Biotechnol* 22:1567–1572.

Table S2. Simulations parameters (related to Figs. 2, 3, and 4) and range of parameters tested for which the main findings are valid (mol == molecules#/cell)

Parameter	Typical values	Range tested	Remarks
Transcription rate for A and B	1 mol · min^{-1}	0.1–10 mol · min^{-1}	In the natural system, A and B have the same transcription rate because they are under the same promoter. The translation rate of B is approximately five times faster than that of A (1). In the simulation transcription and translation were considered as a single process, and the rate was the main control parameter.
Translation rate for A	0.2 · mol/ min /mRNA	0.02–2 · mol/ min /mRNA	
Translation rate for B	1 mol/ min /mRNA	0.1–10 mol/ min /mRNA	
Typical transcription leakage for A and B	10% of the maximal rate	5–15% of the maximal rate	Experimentally evaluated
Cell cycle (during exponential phase)	30 min	20–40 min	Experimentally evaluated
Degradation rate of mRNA	0.1 min^{-1}	0.05–0.2 min^{-1}	The mRNA life time was taken as few minutes (2).
Degradation rate of B	0.3 min^{-1}	0.1–0.6 min^{-1}	Antitoxin proteins are unstable (3). HipB life time was taken as few minutes.
Degradation rate of A and AB	0.02 min^{-1}	0.01–0.04 min^{-1}	The HipA and the complex are assumed to be stable, and the degradation (dilution) is determined by the cell cycle.
Binding rate of AB to the promoter	25 min^{-1} /mol	0.25–250 min^{-1} /mol	From ref. 1, k_{DNA} (which is the ratio between binding and unbinding rates) is approximately 25 mol^{-1}. The exact values of binding and unbinding rates are unknown. Typical values assumed (4). Repression was taken into account only for the *hip* promoter.
Unbinding rate of the bound repressor	1 min^{-1}	0.1–10 min^{-1}	
Association rate of A and B (k_{on})	1 min^{-1} / mol	0.1–10 min^{-1} / mol	Exact values are not known. Typical values assumed (4). Results depend only on the ratio between the rates $k_{AB} = k_{on}/k_{off}$ which can be evaluated from ref. 1 $k_{AB} \sim 1$ mol^{-1}.
Dissociation rate of AB (k_{off})	1 min^{-1}	0.1–10 min^{-1}	
HipA leakage level than prevents growth (A0)	10 mol	1–10	Our experimental results show that leakage expression from tightly repressed promoters (ara and tet) is sufficient to arrest growth in *hipB*$^-$ cells. Typical values above and below leakage measurements (5) were considered.
Persistence definition			Once the growth-arrest time distribution is computed, persisters are defined as cells that are arrested for longer times than two standard deviations away from the mean. This definition is consistent with our experimental results that show the survival of those growth-arrested cells to typical antibiotic treatments of a few hours (Fig. S2)

1 Black DS, Irwin B, Moyed HS (1994) Autoregulation of hip, an operon that affects lethality due to inhibition of peptidoglycan or DNA-synthesis. *J Bacteriol* 176:4081–4091.
2 Bernstein JA, Lin PH, Cohen SN, Lin-Chao S (2004) Global analysis of *Escherichia coli* RNA degradosome function using DNA microarrays. *Proc Natl Acad Sci USA* 101:2758–2763.
3 Gerdes K, Christensen SK, Lobner-Olesen A (2005) Prokaryotic toxin-antitoxin stress response loci. *Nat Rev Microbiol* 3:371–382.
4 Alon U (2007) *An Introduction to Systems Biology: Design Principles of Biological Circuits* (Chapman & Hall/CRC, Boca Raton, FL) pp 241–252.
5 Guzman LM, Belin D, Carson MJ, Beckwith J (1995) Tight regulation, modulation, and high-level expression by vectors containing the arabinose PBAD promoter. *J Bacteriol* 177:4121–4130.

Table S3. Primers table

Name	Sequence
pBADF	5′-ATGCCATAGCATTTTTATCC-3′
3-hipA-int1	5′-TCTCTCTCTCTAGAGCCGGAACCTGATCCCTT-3′
5-cher-INT2	5′-GGATCAGGTTCCGGCTCTAGAGTGAGCAAGGGCGAGGAGGATAACA-3′
3-cher-ext2	5′-TCTCTCTCGCATGCCTGACAGTTACTTGTACAGCTCGT-3′
FWD-mCher-Sph1	5′-TCTCTCTCGCATGCAGGAGGATCCATGGTGAGCAAGG-3′
Rev-mCher-Sph1	5′-TCTCTCTCGCATGCAAGCTTCGAATTCTTACTTGTA-3′
hipp1	CGGATAAACTTGCTGTGGACGTATGACATGATGAGCTTTCAGTGTAGGCTGGAGCTGCTTC
hipp2	AACCGTCCATGCAACCTCAACACATTGCTTTCAACTGCCGATGGGAATTAGCCATGGTCC
c1	TTATACGCAAGGCGACAAGG
c2	GATCTTCCGTCACAGGTAGG
nbl5′	TGTTGAGGGTGGGTATACCT
nb13′	TGTCAGGAAAGGTCAAGAGC
BxbaIF	TCTCTCTCTCTCTAGAATGATGACTTTCAG
BxbaIR	TCTCTCTCTCTCTAGATTACCACTCCAGATT
HECOH	CGGAATTCAAGTTTATCCGCTTAAG
HXHOH1	CCGCTCGAGGCGAAAGTAAATAACA
pZA21-hipA FWD	5′TATATATAGAATTCAGGAGGACTAGCATATGCCTAAACTTGTCA-3′
pZA21-hipAstop REV	5′-ACTGTACAGAATTCGTCACTTACTACCGTATTCTCG-3′